Slave-boson theory of the extended Falicov-Kimball model

P. M. R. Brydon
Max-Planck-Institut für Festkörperforschung, Heisenbergstrasse 1, 70569 Stuttgart, Germany
(Received 13 June 2007; revised manuscript received 8 October 2007; published 9 January 2008)

The extended Falicov-Kimball model, with both an on-site hybridization potential and dispersive narrow band, is examined within the saddle-point approximation to the Kotliar-Ruckenstein [Phys. Rev. Lett. **57**, 1362 (1986)] slave-boson theory. We first set the hybridization potential to zero and find that the phase diagram depends strongly on the orbital structure: for degenerate orbitals, a correlated-insulating state is found at sufficiently strong interaction strengths, whereas a finite orbital energy difference can lead to discontinuous valence transitions. The obtained phase diagram is very sensitive to the presence of a finite hybridization potential. As in Hartree-Fock theory, we find an enhancement of the hybridization by the interorbital Coulomb repulsion. The more precise treatment of correlation effects, however, leads to large deviations from the Hartree-Fock results. In the limit of vanishing hybridization, an excitonic insulator state is only found when the orbitals are degenerate, which restricts this phase to a much smaller parameter space than in other available mean-field theories.

DOI: 10.1103/PhysRevB.77.045109 PACS number(s): 71.30.+h, 71.28.+d, 71.27.+a, 71.10.Fd

I. INTRODUCTION

The Falicov-Kimball model (FKM) was one of the first theoretical attempts to explain valence transitions in mixed-valence systems such as SmB_6 and Ce.[1] In its original form, the model describes a spinless fermion system with conduction (c) electrons interacting via on-site Coulomb repulsion G with narrow band (f) electrons of orbital energy ϵ_f. Within a mean-field theory, it was found that varying G or ϵ_f can produce both continuous and discontinuous changes in the distribution of electrons between these two orbitals, i.e., valence transitions. The FKM is, nevertheless, not a good model of the mixed-valence state as the entirely localized nature of the f electrons is unrealistic.[2] The "classical" nature of the f electrons was subsequently exploited in the reinterpretation of the FKM as a model of charge order in binary alloys.[3]

The central idea behind the FKM, that the interorbital Coulomb repulsion G could be the origin of discontinuous valence transitions, was revisited by several groups who modified the model to account for the quantum nature of the f electrons.[4–6] The so-called extended Falicov-Kimball model (EFKM) allows for the partial delocalization of the f electrons due to the overlap of the orbital wave functions by including a c-f hybridization potential V. Although mean-field impurity models suggested that discontinuous valence transitions were possible in the EFKM,[4,5] weak-coupling studies of the periodic limit found only continuous changes in the orbital populations.[6,7]

An interesting aspect of the Hartree-Fock (HF) solution of the EFKM with on-site hybridization is the existence of an excitonic insulator (EI) phase in the limit $V \to 0$.[5] The EI phase is characterized by a spontaneous hybridization between the c and f bands due to the presence of a nonzero polarization or excitonic average $\langle c^\dagger f \rangle$. This is interpreted as indicating the spontaneous pairing of c electrons with f holes, forming an excitonic condensate. Introduced independently by Keldysh and Kopaev[8] and des Cloizeaux,[9] the EI is an important concept in the study of semimetal-semiconductor transitions. A spontaneous hybridization between the nested portions of the Fermi surface has proven to be a particularly useful description of the spin density-wave phase of Cr-based alloys;[10] a similar scenario has also recently been proposed as an explanation for the orbital ordering in $LaMnO_3$.[11] Unambiguous examples of the EI phase remain rare, however, with only two likely candidates, the alloys $Sm_{0.9}La_{0.1}S$ and $TmSe_{0.45}Te_{0.55}$, thus far discovered.[12] This indicates that the conditions for an EI phase must be significantly more restrictive than those encountered in the usual phenomenological Hamiltonian description.

The EFKM is the only "standard" tight-binding model of correlated electron systems that has been claimed to display an EI phase.[5] It has attracted much attention due to the proposal by Portengen *et al.* that the spontaneous excitonic average in the EFKM could be interpreted as evidence of electronic ferroelectricity.[13] Although a variety of more sophisticated treatments[14,15] or more general mean-field theories[16,17] have failed to find the EI phase, the presence of a finite f-electron hopping can stabilize the EI state in the strong-coupling regime.[18,19] Whether or not the EI phase is realized, it seems likely that in the EFKM with $V \neq 0$, the interorbital Coulomb interaction will induce a large "excitonic" renormalization of the bare on-site hybridization potential.[16,17]

The continuing controversy regarding the EI phase in the EFKM and the larger question about the rarity of EI phases motivate us to study the EFKM using a more advanced analytical technique than the weak-coupling methods hitherto employed. A particularly useful analytic approach for obtaining the ground state properties of strongly correlated lattice models is the slave-boson (SB) mean-field theory developed by Kotliar and Ruckenstein.[20] This is superior to HF mean-field theory as it accounts for the renormalization of the quasiparticle weight by the interactions, similar to a Fermi-liquid description. It is also of interest to study the SB solution of the EFKM for the possible application to multiband Hubbard

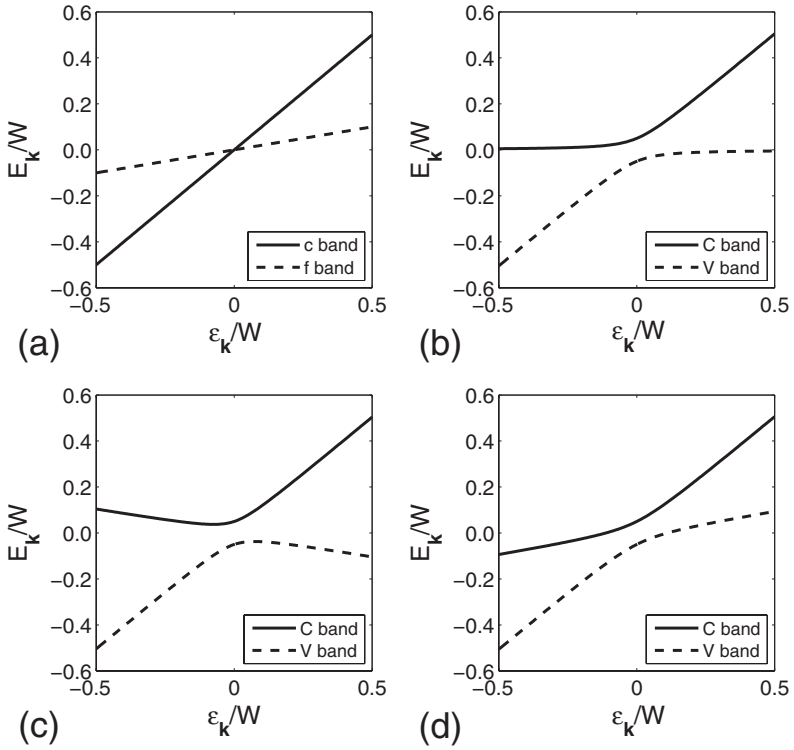

FIG. 1. Different band scenarios for the noninteracting EFKM with $\epsilon_f=0$. W is the bandwidth of the bare c-electron band. (a) c- and f-electron bands for $t_{ff}=0.2$ and $V=0.0$. (b) C and V bands for $t_{ff}=0.0$ and $V=0.05W$. (c) C and V bands for $t_{ff}=-0.2$ and $V=0.05W$. (d) C and V bands for $t_{ff}=0.2$ and $V=0.05W$.

models:[21] in general, the presence of an on-site hybridization makes it impossible to apply the usual SB formalism as the atomic Hamiltonian cannot then be written only in terms of density operators. Although generalizations of the SB mean-field theory have been developed to cope with these difficulties,[22] the effect of interorbital interactions on the hybridization is still poorly understood. We can obtain some insight into this situation by studying the EFKM with a finite hybridization, as this can be treated within the usual SB formulation.

In this paper, we examine the EFKM at zero temperature ($T=0$) and half-filling (i.e., one electron per lattice site) using the Kotliar-Ruckenstein SB theory. In Sec. II, we outline the construction of the mean-field SB Hamiltonian and also review the usual HF solution. In both cases, we consider only uniform ground states. The results are presented in Sec. III. The solution of the $V=0$ system (Sec. III A) is found to be very sensitive to the orbital structure. For degenerate c and f orbitals, a Brinkman-Rice-like insulating state is found at sufficiently large interaction strength; for nondegenerate orbitals, discontinuous valence transitions can be found. The orbital structure also determines the behavior of the EFKM with $V\neq 0$ and a holelike or dispersionless f band (Sec. III B): for degenerate orbitals, the SB solution resembles closely the predictions of the HF theory; for nondegenerate orbitals, the more accurate treatment of correlation effects in the SB theory produces strong deviations from the HF results. A first-order metal-insulator transition is found with increasing interaction strength for an electronlike f band (Sec. III C), in contrast to the second-order transitions found in HF theory. Within the SB treatment of the model, the EI phase is only possible when the c and f orbitals are degenerate (Sec. III D). We conclude in Sec. IV with a summary of our results and outlook for further work.

II. SLAVE-BOSON HAMILTONIAN

The Hamiltonian for the EFKM is written

$$\mathcal{H}_{\mathrm{EFKM}}=\sum_{\mathbf{k}}\epsilon_{\mathbf{k}}\{c_{\mathbf{k}}^{\dagger}c_{\mathbf{k}}+t_{ff}f_{\mathbf{k}}^{\dagger}f_{\mathbf{k}}\}+\epsilon_f\sum_j f_j^{\dagger}f_j+V\sum_j\{c_j^{\dagger}f_j+\mathrm{H.c.}\}+G\sum_j n_j^c n_j^f, \quad (1)$$

where $c_{\mathbf{k}}$ (c_j) and $f_{\mathbf{k}}$ (f_j) are the annihilation operators in momentum (real) space for the c and f electrons, respectively. The c-electron dispersion is $\epsilon_{\mathbf{k}}$; the f-electron dispersion is assumed to be a multiple $|t_{ff}|<1$ of the c-electron dispersion. In this work, we consider holelike ($t_{ff}<0$), dispersionless ($t_{ff}=0$), and electronlike ($t_{ff}>0$) f electron bands. The different band dispersions $E_{\mathbf{k}}$ in the noninteracting limit are shown as functions of $\epsilon_{\mathbf{k}}$ in Fig. 1. For $V\neq 0$, the bands are of mixed c and f character: we refer to the upper and lower bands as the conduction (C) and valence (V) bands, respectively. For $t_{ff}\leqslant 0$, there is always a finite gap between the C and V bands when $V\neq 0$, and so at half-filling, the noninteracting ground state is insulating. In contrast, for sufficiently large $t_{ff}>0$, there is an overlap between the C and V bands, and so the ground state is metallic at half-filling.

In the absence of a hybridization potential between the c and f states, we may immediately apply the SB technique. In the case when $V\neq 0$, however, the SB technique cannot be straightforwardly applied as the atomic Hamiltonian [obtained by neglecting the first term on the right-hand side of Eq. (1)] is not diagonal in the electron occupation operators.[22] To proceed, we rewrite the system in terms of a diagonal on-site basis

$$b_j = \alpha c_j + \beta f_j, \quad a_j = \beta c_j - \alpha f_j, \tag{2}$$

where

$$\alpha = \frac{\mathrm{sgn}(\epsilon_f + 0^+)}{\sqrt{2}}\left[1 + \sqrt{1 - \frac{4V^2}{4V^2 + \epsilon_f^2}}\right]^{1/2}, \tag{3}$$

$$\beta = -\frac{1}{\sqrt{2}}\left[1 - \sqrt{1 - \frac{4V^2}{4V^2 + \epsilon_f^2}}\right]^{1/2}. \tag{4}$$

Note that $\mathrm{sgn}(x+0^+)=1(-1)$ for $x \geqslant 0 (x<0)$. In terms of the a and b operators, we can hence rewrite the Hamiltonian

$$\begin{aligned}\mathcal{H}_{\mathrm{EFKM}} = \sum_{\mathbf{k}} \epsilon_{\mathbf{k}} \{ & (\alpha^2 + t_{ff}\beta^2) b_{\mathbf{k}}^\dagger b_{\mathbf{k}} + (\beta^2 + t_{ff}\alpha^2) a_{\mathbf{k}}^\dagger a_{\mathbf{k}} \\ & + (1 - t_{ff})\alpha\beta [a_{\mathbf{k}}^\dagger b_{\mathbf{k}} + b_{\mathbf{k}}^\dagger a_{\mathbf{k}}]\} \\ & + \epsilon_a \sum_j a_j^\dagger a_j + \epsilon_b \sum_j b_j^\dagger b_j + G \sum_j n_j^a n_j^b, \end{aligned} \tag{5}$$

where $\epsilon_b = \epsilon_f \beta^2 + 2\alpha\beta V$ and $\epsilon_a = \epsilon_f \alpha^2 - 2\alpha\beta V$. Although there is a hybridization between the a and b orbitals in Eq. (5), it is proportional to $\epsilon_{\mathbf{k}}$ and, hence, it is now a kinetic term; in contrast, the local Hamiltonian is diagonal. This allows us to proceed to unambiguously assign Kotliar-Ruckenstein slave-boson fields to the different occupancy states of each lattice site.

We adopt the Kotliar-Ruckenstein SB theory by introducing the auxiliary bosonic fields e_j, s_{aj}, s_{bj}, and d_j, which, respectively, destroy the empty, singly occupied a orbital, singly occupied b orbital, and doubly occupied atomic configurations at site j. The fermionic Hamiltonian is then written in terms of quasifermions $\tilde{a}$ and $\tilde{b}$ using the identification

$$a_j = z_{aj} \tilde{a}_j, \tag{6}$$

$$b_j = z_{bj} \tilde{b}_j, \tag{7}$$

where

$$\begin{aligned} z_{a(b)j} = & (1 - d_j^\dagger d_j - s_{a(b)j}^\dagger s_{a(b)j})^{-1/2} (s_{b(a)j}^\dagger d_j + e_j^\dagger s_{a(b)j}) \\ & \times (1 - s_{b(a)j}^\dagger s_{b(a)j} - e_j^\dagger e_j)^{-1/2}. \end{aligned} \tag{8}$$

The physical interpretation of the bosonic fields implies that the following equations are satisfied at each site:

$$1 = e_j^\dagger e_j + s_{aj}^\dagger s_{aj} + s_{bj}^\dagger s_{bj} + d_j^\dagger d_j, \tag{9}$$

$$\tilde{a}_j^\dagger \tilde{a}_j = s_{aj}^\dagger s_{aj} + d_j^\dagger d_j, \tag{10}$$

$$\tilde{b}_j^\dagger \tilde{b}_j = s_{bj}^\dagger s_{bj} + d_j^\dagger d_j. \tag{11}$$

These constraints are respectively enforced by the constraint fields λ_j, Λ_{aj}, and Λ_{bj}, which enter as Lagrangian multipliers.

A mean-field theory is constructed by replacing the boson and constraint fields by spatially uniform time-invariant fields, i.e., $e_j \to e$, $s_{bj} \to s_b$, etc. This yields the Hamiltonian

$$\begin{aligned} \mathcal{H}_{\mathrm{SB}} = & \sum_{\mathbf{k}} \epsilon_{\mathbf{k}} \{ z_b^2 (\alpha^2 + t_{ff}\beta^2) \tilde{b}_{\mathbf{k}}^\dagger \tilde{b}_{\mathbf{k}} + z_a^2 (\beta^2 + t_{ff}\alpha^2) \tilde{a}_{\mathbf{k}}^\dagger \tilde{a}_{\mathbf{k}} \\ & + z_a z_b (1 - t_{ff}) \alpha\beta [\tilde{a}_{\mathbf{k}}^\dagger \tilde{b}_{\mathbf{k}} + \tilde{b}_{\mathbf{k}}^\dagger \tilde{a}_{\mathbf{k}}]\} + (\epsilon_a + \Lambda_a) \sum_j \tilde{a}_j^\dagger \tilde{a}_j \\ & + (\epsilon_b + \Lambda_b) \sum_j \tilde{b}_j^\dagger \tilde{b}_j + NGd^2 - N\lambda(e^2 + s_a^2 + s_b^2 + d^2 - 1) \\ & - N\Lambda_a (s_a^2 + d^2) - N\Lambda_b (s_b^2 + d^2), \end{aligned} \tag{12}$$

where

$$z_{a(b)} = (1 - d^2 - s_{a(b)}^2)^{-1/2} (d s_{b(a)} + e s_{a(b)}) (1 - s_{b(a)}^2 - e^2)^{-1/2} \tag{13}$$

are the band-renormalization factors. We work throughout at half-filling

$$1 = \frac{1}{N} \sum_j \{ \langle \tilde{a}_j^\dagger \tilde{a}_j \rangle + \langle \tilde{b}_j^\dagger \tilde{b}_j \rangle \} = \frac{1}{N} \sum_j \{ \langle c_j^\dagger c_j \rangle + \langle f_j^\dagger f_j \rangle \} \tag{14}$$

as in this limit it may be explicitly demonstrated by extremization of the free energy that $z_a = z_b = z$.

The quasifermion component of the Hamiltonian Eq. (12) can be straightforwardly diagonalized. For finite c-f hybridization, we have the quasifermion C and V bands

$$\begin{aligned} E_{\mathbf{k}}^{\mathrm{C(V)}} = & \frac{1}{2} \{ (1 + t_{ff}) z^2 \epsilon_{\mathbf{k}} + \tilde{\epsilon}_a + \tilde{\epsilon}_b \\ & + (-) \sqrt{[(1 - t_{ff}) z^2 \epsilon_{\mathbf{k}} + \tilde{\epsilon}_a - \tilde{\epsilon}_b]^2 + 4\tilde{V}^2} \}, \end{aligned} \tag{15}$$

where

$$\tilde{\epsilon}_a = \alpha^2 (\epsilon_b + \Lambda_b) + \beta^2 (\epsilon_a + \Lambda_a), \tag{16}$$

$$\tilde{\epsilon}_b = \beta^2 (\epsilon_b + \Lambda_b) + \alpha^2 (\epsilon_a + \Lambda_a), \tag{17}$$

$$\tilde{V} = \alpha\beta (\epsilon_a + \Lambda_a - \epsilon_b - \Lambda_b). \tag{18}$$

Note the renormalization of the hybridization by the constraint fields: this is the equivalent of the excitonic enhancement seen in HF studies. Of particular importance then is the so-called excitonic average, defined as

$$\begin{aligned} \Delta = \frac{1}{N} \sum_j \langle c_j^\dagger f_j \rangle = & \frac{\alpha\beta}{N} \sum_j \{ \langle \tilde{b}_j^\dagger \tilde{b}_j \rangle - \langle \tilde{a}_j^\dagger \tilde{a}_j \rangle \} \\ & + \frac{\beta^2 - \alpha^2}{2N} \sum_j \{ \langle \tilde{a}_j^\dagger \tilde{b}_j \rangle + \langle \tilde{b}_j^\dagger \tilde{a}_j \rangle \}. \end{aligned} \tag{19}$$

If Δ remains finite as $V \to 0$, the system has an instability toward the EI phase.

The familiar SB self-consistency conditions are obtained by minimizing the free energy with respect to the SB fields while maximizing with respect to the constraint fields, the so-called saddle-point approximation. The free energy may be calculated analytically in the case of a rectangular density of states (DOS)

$$\rho(\omega) = \begin{cases} 1/W, & |\omega| < W/2 \\ 0, & |\omega| > W/2, \end{cases} \tag{20}$$

where the DOS of the bare c and f bands is respectively $\rho_c(\omega)=\rho(\omega)$ and $\rho_f(\omega)=|t_{ff}|^{-1}\rho(t_{ff}^{-1}[\omega-\epsilon_f])$. Although the details of the self-consistent solutions will change upon adopting a more realistic band structure, the rectangular DOS is convenient for studying the generic behavior of the model.

A. Hartree-Fock theory

For comparison, we briefly discuss the usual HF solution of the EFKM.[6] An effective single-particle Hamiltonian may be derived from Eq. (1) by replacing the interaction term by coupling to mean fields

$$G\sum_j n_j^c n_j^f \approx Gn_c\sum_j n_j^f + Gn_f\sum_j n_j^c - G\Delta\sum_j \{c_j^\dagger f_j + \text{H.c.}\} - NGn_cn_f + NG\Delta^2, \tag{21}$$

where the HF variational parameters n_c, n_f, and Δ are respectively the c-electron concentration, the f-electron concentration, and the excitonic average defined in Eq. (19). Unlike the SB theory, the decoupling scheme Eq. (21) is usually only a good approximation when the interaction strength is much less than the bandwidth, and so it is not *a priori* clear that it is appropriate for localized f electrons in the EFKM at any value of the coupling.[5] Substituting Eq. (21) into Eq. (1), we obtain the mean-field Hamiltonian

$$\mathcal{H}_{HF} = \sum_{\mathbf{k}} \epsilon_{\mathbf{k}}\{c_{\mathbf{k}}^\dagger c_{\mathbf{k}} + t_{ff} f_{\mathbf{k}}^\dagger f_{\mathbf{k}}\} + \tilde{\epsilon}_c\sum_j c_j^\dagger c_j + \tilde{\epsilon}_f\sum_j f_j^\dagger f_j + \tilde{V}\sum_j \{c_j^\dagger f_j + \text{H.c.}\} - NGn_cn_f + NG\Delta^2, \tag{22}$$

where $\tilde{\epsilon}_c=Gn_f$, $\tilde{\epsilon}_f=\epsilon_f+Gn_c$, and $\tilde{V}=V-G\Delta$. The self-consistency equations for the HF parameters are easily found by diagonalization of the Hamiltonian Eq. (22), see, for example, Ref. 6. As for the SB results, we calculate the self-consistency equations analytically using the rectangular DOS Eq. (20).

Since the SB parameters are related to the concentration of sites in a given orbital configuration, we can also obtain HF values of these parameters directly from the HF wave function $|\Psi_{HF}\rangle$. Explicitly, we have

$$d_{HF}^2 = \frac{1}{N}\sum_j \langle\Psi_{HF}|n_j^c n_j^f|\Psi_{HF}\rangle = n_c(1-n_c) - \Delta^2, \tag{23}$$

$$s_{bHF}^2 = \frac{1}{N}\sum_j \langle\Psi_{HF}|\alpha^2 n_j^c + \beta^2 n_j^f + \alpha\beta\{c_j^\dagger f_j + f_j^\dagger c_j\}|\Psi_{HF}\rangle - d_{HF}^2 = \beta^2 + (\alpha^2-\beta^2)n_c - n_c(1-n_c) + 2\alpha\beta\Delta + \Delta^2, \tag{24}$$

$$s_{aHF}^2 = \frac{1}{N}\sum_j \langle\Psi_{HF}|\beta^2 n_j^c + \alpha^2 n_j^f - \alpha\beta\{c_j^\dagger f_j + f_j^\dagger c_j\}|\Psi_{HF}\rangle - d_{HF}^2 = \alpha^2 + (\beta^2-\alpha^2)n_c - n_c(1-n_c) - 2\alpha\beta\Delta + \Delta^2, \tag{25}$$

$$e_{HF}^2 = 1 - s_{aHF}^2 - s_{bHF}^2 - d_{HF}^2 = n_c(1-n_c) - \Delta^2. \tag{26}$$

III. RESULTS

As we work throughout at $T=0$ and fixed particle number, we perform the extremization for the SB theory upon the ground state energy per site $E=\langle\mathcal{H}_{SB}\rangle/N$. This is calculated analytically using the density of states Eq. (20). The physical values of the SB and constraint fields are then obtained by determining the saddle point of the ground state energy, which requires that we solve the equations

$$\frac{\partial E}{\partial e} = \frac{\partial E}{\partial s_a} = \frac{\partial E}{\partial s_b} = \frac{\partial E}{\partial d} = \frac{\partial E}{\partial \lambda} = \frac{\partial E}{\partial \Lambda_a} = \frac{\partial E}{\partial \Lambda_b} = 0. \tag{27}$$

We employ a multidimensional Newton-Raphson technique to solve Eq. (27). To obtain the HF results, we iterate the self-consistency equations until a desired accuracy is obtained.

A. $V=0$, $t_{ff}\neq 0$

We begin by examining the EFKM without hybridization. Mathematically, this limit is very closely related to the uniform Gutzwiller and SB solutions of the Hubbard model in a magnetic field:[20,23] by identifying the longitudinal magnetic field with ϵ_f, the expression for E in the two models is of the same form, although the effective bandwidth of the EFKM is smaller by a factor $(1+|t_{ff}|)/2$. This similarity implies that within the SB approximation and assuming uniform ground states, the behavior of the EFKM is a charge analog of the paramagnetic Hubbard model. In particular, there is a localization transition at $\epsilon_f=0$, and at sufficiently small $\epsilon_f\neq 0$, a first-order valence transition occurs. This is displayed in our plots of the SB fields in Fig. 2. We do not discuss the HF predictions for the EFKM with $V=0$ as this only involves the renormalization of the orbital energies, see Eq. (22).

At $\epsilon_f=0$, there is a second-order transition from the low-G metallic (M) state into a Brinkman-Rice-like correlated-insulator (CI) phase at $G/W=1+|t_{ff}|$. This is a localization transition, as the band-renormalization factor z^2 vanishes in the CI phase. In this state, every site is singly occupied with equal probability by either a c or f electron, reflected in the limiting values $s_c=s_f=1/\sqrt{2}$ in Fig. 2(c) and $d=0$ in Fig. 2(b). As implied by the equality of c- and f-electron populations, the difference between the effective c and f energy levels, $\Lambda_c-\Lambda_f$, is zero for all G.

For any finite ϵ_f, the high-G state is an integer valence state with filled c band (f band) for $\epsilon_f>0$ ($\epsilon_f<0$). This filled-band (FB) state is not localized, so we have $z=1$ [Fig. 2(a)]; at $\epsilon_f>0$, it is also characterized by $s_c=1$ and $d=e=s_f=0$ [Figs. 2(b) and 2(c)]. As G is increased, $\Lambda_c-\Lambda_f$ decreases to the fixed value $\epsilon_f-\frac{1}{2}(1+|t_{ff}|)W$ in the FB phase: this raises the effective f level so that the bottom of the f band just touches the top of the c band.

The transition into the FB phase from the M phase is an example of a valence transition, as it is a transition from a state with mixed valence (i.e., nonzero c and f populations) into a state with integer occupation of the orbitals. This transition is qualitatively different at small and large $|\epsilon_f|$. For small $|\epsilon_f|$, the FB state is reached from the M phase by a first-order transition, which is the charge analog of the meta-

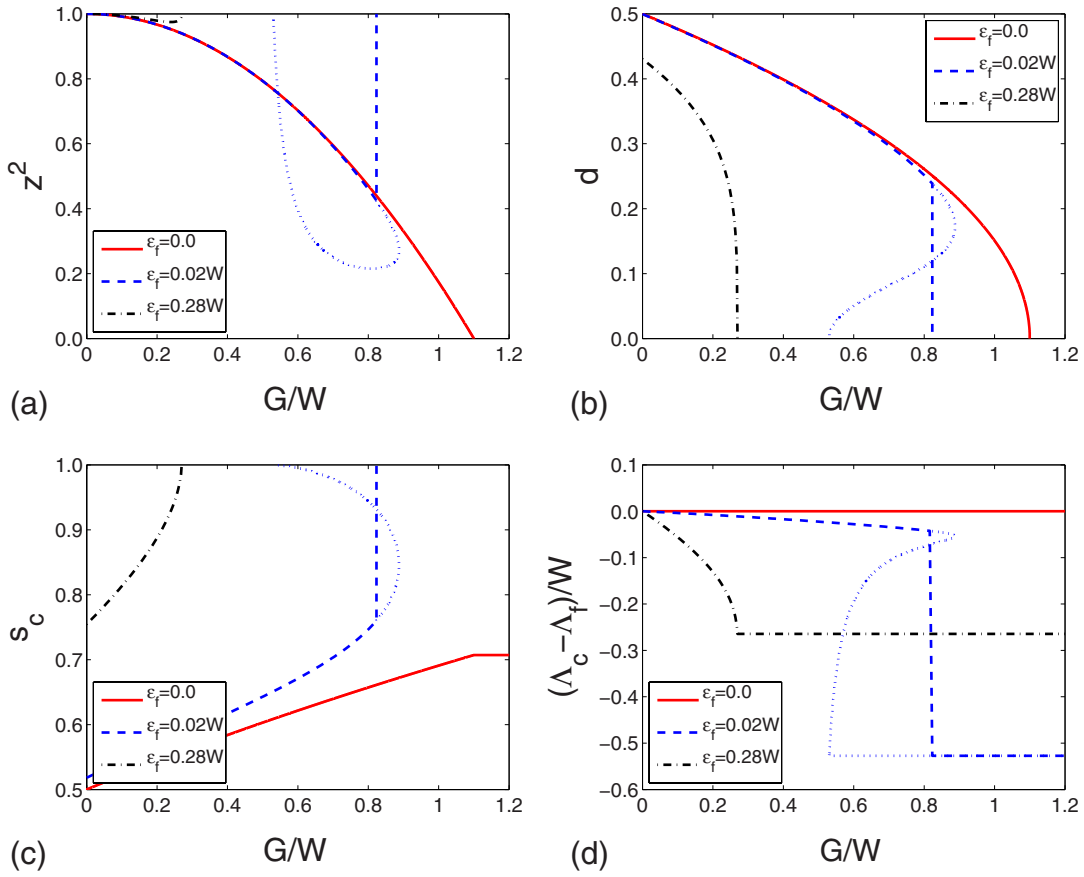

FIG. 2. (Color online) Variation of the SB parameters with G for $t_{ff}=0.1$, $V=0$, and various values of ϵ_f. The metastable solution for $\epsilon_f=0.02W$ is given by the dotted line. (a) Band-renormalization factor z^2. (b) SB field d. (c) SB field s_c. (d) Constraint field $\Lambda_c-\Lambda_f$.

magnetic transition in the SB treatment of the Hubbard model. Within the region where both FB and M solutions of Eq. (27) are possible, the stable ground state is defined to be the one with the lower energy. Multiple solutions are only found within the region bounded between the dashed lines and $\epsilon_f=0$ in Fig. 3, with the metastable state indicated within the brackets following the stable state. The FB and M phases have equal energy along the dotted line. As $|\epsilon_f|$ is increased, the boundaries of metastability of the FB and M phases converge together at $|\epsilon_f|\approx 0.25W$, beyond which we find that the FB and M phases are separated by a second-order transition. Further increasing $|\epsilon_f|$, the line of second-order transitions intersects the line $G=0$ at $|\epsilon_f|=\frac{1}{2}(1+t_{ff})W$: for $|\epsilon_f|>\frac{1}{2}(1+t_{ff})W$, there is no overlap between the c and f bands in the $G=0$ limit and so the system is always in the FB state.

B. $V\neq 0$, $t_{ff}\leqslant 0$

The presence of a finite hybridization potential has a dramatic effect on the EFKM with $t_{ff}\leqslant 0$, as the system is then in an insulating state at $G=0$ as illustrated in Figs. 1(b) and 1(c). We find, however, that in the interacting system, the cases $\epsilon_f=0$ and $\epsilon_f\neq 0$ are distinguished by very different behaviors in the $V\to 0$ limit.

As shown in Fig. 4(a), for $\epsilon_f=0$ and any finite V, the band-renormalization factor z^2 decreases as G is increased, but eventually goes through a minimum before asymptoting

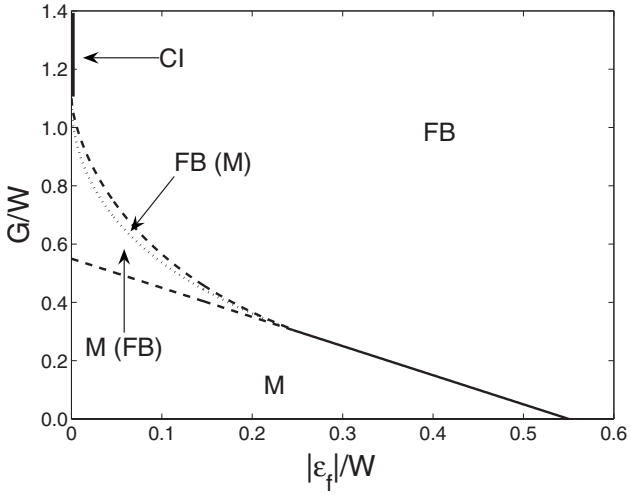

FIG. 3. Phase diagram for the EFKM in the G-ϵ_f plane. We have $|t_{ff}|=0.1$ and $V=0$. At $\epsilon_f=0$, we have a second-order transition between the M phase and the CI phase. The limits of metastability of the FB and M phases are given by the dotted lines; along the dashed line, the two phases have equal energy. Where metastable state exists, it follows after the stable state in brackets. The solid line for $|\epsilon_f|\gtrsim 0.25W$ gives the second-order transition between the M and FB phases.

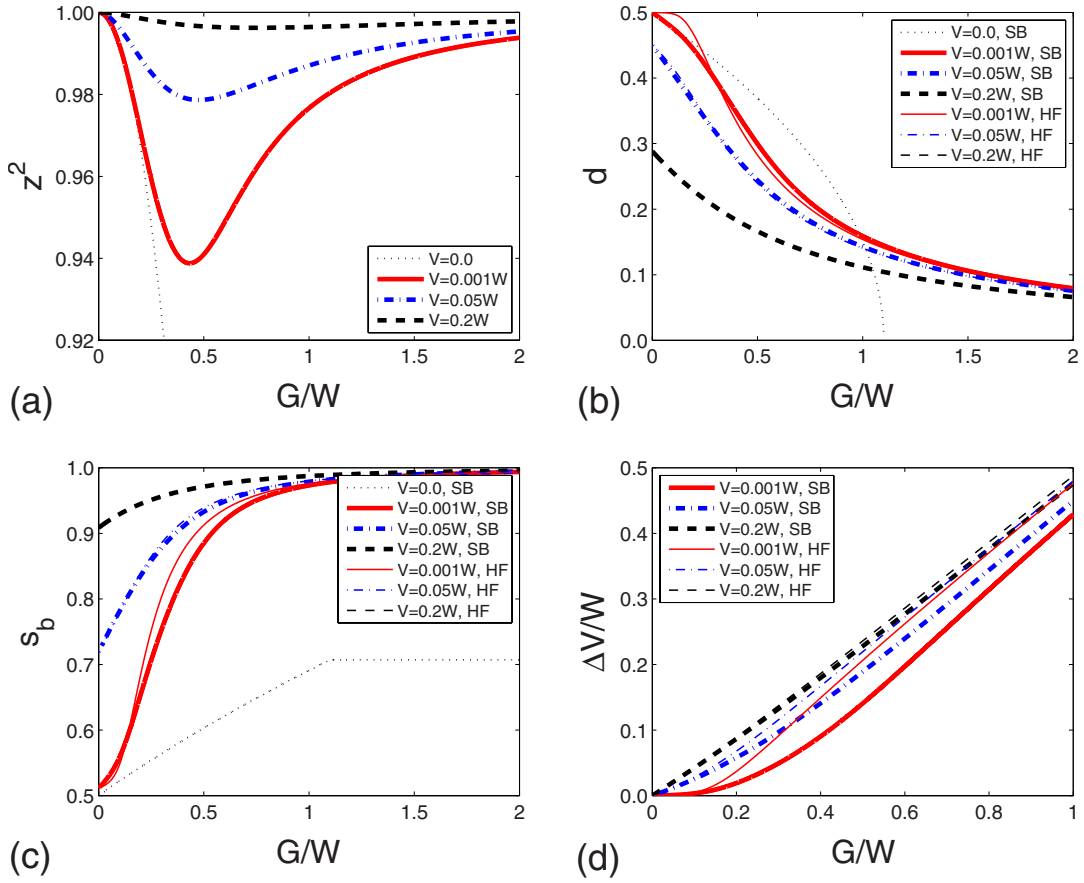

FIG. 4. (Color online) Variation of the SB parameters with G for $t_{ff}=-0.1$, $\epsilon_f=0$, and various values of V. In (b)–(d), the thick lines indicate the SB solution, while the thin lines of the same style and color indicate the corresponding Hartree-Fock solution. (a) Band-renormalization factor z^2. (b) SB field d. (c) SB field s_b. (d) Change in hybridization ΔV.

to unity. For $V \ll W$, z^2 closely follows the band renormalization in the $V=0$ system until $G \approx 0.2W$, where the curvature changes and a minimum value is subsequently reached at $G \approx 0.4W$. This has been checked down to $V=10^{-5}W$ (not shown), which is found to give almost identical results to the system with $V=10^{-3}W$. This has an important implication: we do not recover the results of Sec. III A in the limit $V \to 0$, indicating that there is a spontaneous hybridization in the $V=0$ system. We will discuss this EI phase in more detail in Sec. III D. Although the minimum in z^2 suggests a crossover between two distinct regimes, this interpretation has to be used with caution: since the depth of the minimum decreases with increasing V, the difference between the low- and high-G regimes becomes less pronounced.

To understand the nature of the low- and high-G regimes, in Figs. 4(b)–4(d), we compare the SB and HF results for d, s_b, and the excitonic enhancement of the hybridization $\Delta V = \tilde{V} - V$. For small V, the SB results differ considerably from the HF results for $G \lesssim 1$, although with increasing G, the results of the two theories converge, which indicates that the physics of the high-G regime is HF-like. This is consistent with the $G \to \infty$ limit of z^2, which is unity as in a HF theory. This HF-like behavior is observed for all G at sufficiently large V: for $V=0.2W$, the SB and HF results for s_b and d are almost identical for all G, although there is still a noticeable difference in the G dependence of ΔV. This is consistent with the very shallow minimum in z^2 observed in Fig. 4(a).

For $G \lesssim 0.2W$ and $V=0.001W$, the SB result for d decreases linearly with G, closely following the $V=0$ results [Fig. 4(b)]. This is in contrast to the HF theory, which predicts that d differs from its noninteracting value by $\propto \Delta^2 \sim \exp(-2W/G)$ in this regime [see Eq. (23)]. The value of s_b, however, does not follow the $V=0$ results over the same range: this is due to the greater sensitivity of s_b to the magnitude of the hybridization, as can be seen by examining the evolution of the $G=0$ values as V is decreased. Further lowering V, we indeed find that the $V=0$ results are tracked in the low-G regime (not shown). These results, along with the variation of z^2, clearly indicate the importance of correlations beyond HF theory at small G and V.

The different treatment of the on-site Coulomb interaction in the two theories is essential to understanding the divergence between the HF and SB results. In the HF theory, the Coulomb interaction indirectly affects the concentration of doubly occupied sites (d^2) through the renormalization of the band parameters; in this case, only the hybridization (at $\epsilon_f = 0$, the renormalization of the orbital energies is identical). In the SB theory, however, the penalty for double occupancy of a site is also explicitly taken into account in the mean-field Hamiltonian Eq. (12) by the Gd^2 term. Thus, for $G, V \ll W$, when the Coulomb renormalization of the hybridization is

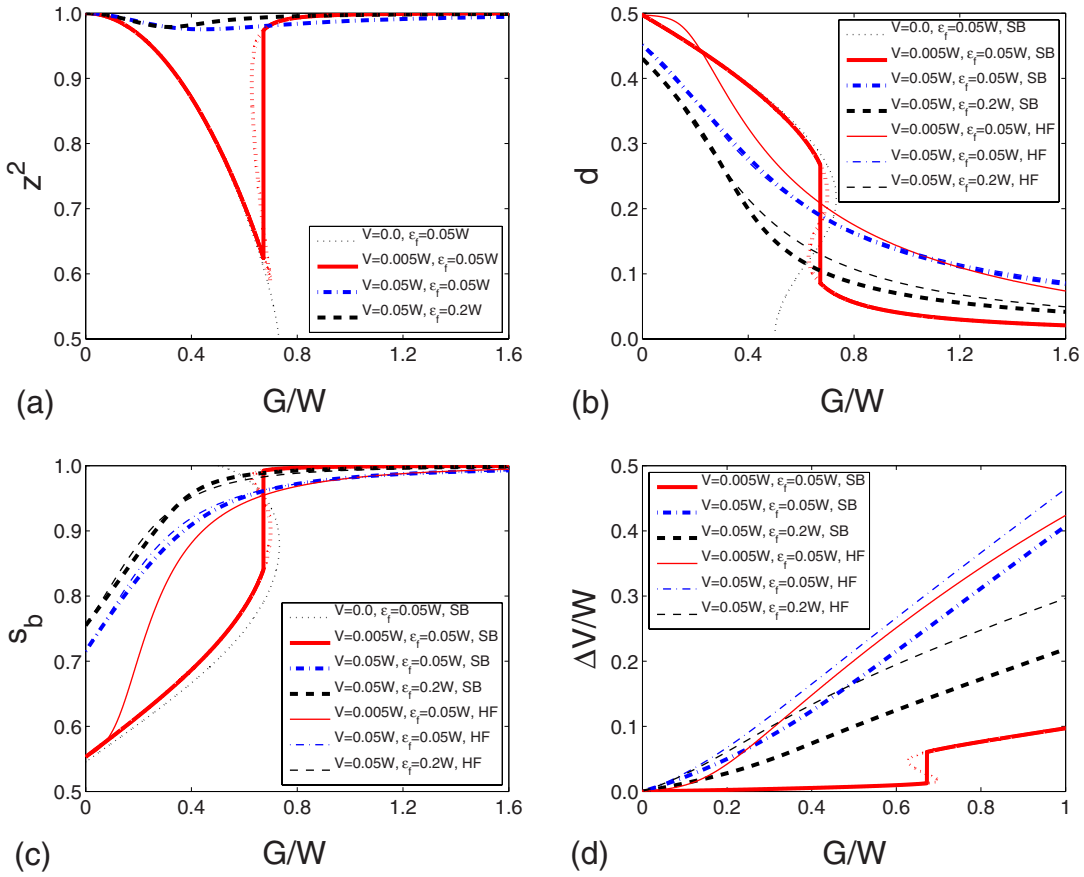

FIG. 5. (Color online) Variation of the SB parameters with G and V for $t_{ff}=-0.1$ and $\epsilon_f \neq 0$. In (b)–(d), the thick lines indicate the SB results, while the thin lines of the same style and color indicate the Hartree-Fock results. For the $\epsilon_f=0.05W$, $V=0.005W$ SB result, the metastable solution is given by the thick dotted line. (a) Band-renormalization factor z^2. (b) SB field d. (c) SB field s_b. (d) Change in hybridization ΔV.

exponentially small in both theories, the SB theory, nevertheless, predicts that d^2 shows a reduction $\propto G$, whereas the HF theory has only $\sim\exp(-2W/G)$ reduction. At $G \gtrsim W$, where the renormalization of the hybridization is large and grows linearly with G for both theories, the G dependences of the SB and HF predictions for d are almost equal. The interesting conclusion that can be drawn is that within the SB theory, the on-site Coulomb repulsion is less important to the physics than the renormalization of V in the high-G regime. That is, the excitonic enhancement of the hybridization gap compensates for the energy penalty due to the finite concentration of doubly occupied sites.

The G dependence of the SB fields for $\epsilon_f \neq 0$ is qualitatively similar to the $\epsilon_f=0$ results for sufficiently large V, but as V is reduced, they converge toward the $V=0$ results of Sec. III A. This can clearly be seen for the $V=0.005W$, $\epsilon_f=0.05W$ line in Figs. 5(a)–5(c), which closely follows the $V=0$ curve almost until the valence transition is reached at $G \approx 0.7W$. Although d does not vanish at higher G when $V \neq 0$, it is heavily suppressed below its value in the HF theory. Intermediate between the low- and high-G regimes, there is a small range of G values for which two solutions exist, implying a discontinuous evolution from the low- to the high-G regimes. Unlike the $\epsilon_f=0$ case [Fig. 4(c)], for $G \lesssim 0.7W$, the G dependence of s_b is very similar to that of the $V=0$ results [thin dotted line in Fig. 5(c)]. The renormalization of the hybridization remains small in the low-G regime, but it is much larger and grows linearly with G beyond the jump discontinuity. This linear increase is, nevertheless, slower than in the HF theory for all finite ϵ_f and V. This can be explained by the V dependence of the hybridization enhancement

$$\Delta V = \frac{|V|}{\sqrt{4V^2+\epsilon_f^2}}(\Lambda_a - \Lambda_b). \tag{28}$$

The prefactor in Eq. (28) arises from the transformation to the a-b basis and has important consequences for the SB theory of the EFKM. For $\epsilon_f=0$, we see that the prefactor is independent of V, and we obtain close correspondence with the HF results. For finite ϵ_f, however, the prefactor vanishes as $V \to 0$, whereas $\Lambda_a - \Lambda_b$ remains finite. This result implies that within the SB theory, there is no spontaneous hybridization if $\epsilon_f \neq 0$, which is in strong contradiction to the HF theory, where the EI phase is stable at $T=0$ for a finite range of ϵ_f.[5,13] Indeed, for $\epsilon_f \neq 0$, the SB and HF theories are only in agreement when $V \gg |\epsilon_f|$.

The evolution of the model with decreasing V is shown in the phase diagram in Fig. 6. We classify the low- and high-G regimes as the band-narrowed insulator (BNI) and the exci-

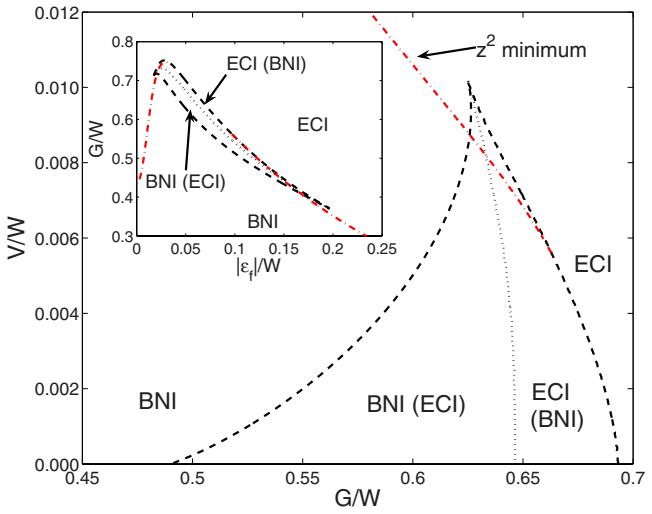

FIG. 6. (Color online) Phase diagram in the G-V plane for $t_{ff}=-0.1$ and $\epsilon_f=0.06W$. At high G, we have an ECI, whereas at low G, the BNI is realized. The dashed lines bound the region where both BNI and ECI solutions are found, with the metastable state written in brackets. Along the dotted line, the BNI and ECI solutions have equal energy. The red dot-dash line indicates the location of the minimum in z^2: within the region where both BNI and ECI solutions are found, this refers only to the BNI regime. The inset shows the phase diagram in the G-ϵ_f plane for $t_{ff}=-0.1$ and $V=0.005W$. Lines are the same as in the main figure.

tonically correlated insulator (ECI), respectively. The former reflects the reduced $z^2<1$, which is characteristic of the $G<W$ solution when $V\ll 0.1W$, whereas the latter is due to the substantial excitonic renormalization of the hybridization in the high-G regime with characteristic $\tilde{V}\propto G$ dependence. These designations are most useful where the evolution from the BNI to the ECI with increasing G is discontinuous. When there is no such discontinuity separating the low- and high-G regimes, the minimum in z^2 can serve as an approximate boundary. We emphasize that the BNI and ECI are not distinct *phases* of the EFKM, as both are insulators and there is no order parameter to distinguish between the two. Rather, they should be regarded as labeling regions of the phase diagram according to the dominant effect of the correlations. We see from the inset that at $V=0.005W$, multiple solutions are possible within the thin region enclosed by the dashed lines, with the metastable state indicated in brackets. The inset in Fig. 6 can be directly compared to Fig. 3. As seen in the main figure, the region of multiple solutions expands to fit the $V=0$ boundaries as V is decreased, with the BNI (ECI) regimes evolving into the M (FB) phase in the $V=0$ limit. Note the sensitivity of the region of multiple solutions to a finite V: this vanishes completely for $V\gtrsim 0.01W$. We conclude that $V\neq 0$ strongly suppresses any tendency to phase separation in the EFKM.

C. $V\neq 0$, $t_{ff}>0$

The behavior of the EFKM with $V\neq 0$ and $t_{ff}>0$ is qualitatively different from that for $t_{ff}\leqslant 0$. For sufficiently small V, the $t_{ff}>0$ noninteracting ground state is metallic, as shown in Fig. 1(d). As G is increased, however, the excitonic renormalization of the hybridization eventually opens a gap and the system is then in the ECI phase. In Fig. 7, we present representative examples of the different behaviors displayed by the EFKM at constant $V=0.05W$ and $\epsilon_f=0$. The behavior of the system for $\epsilon_f\neq 0$ is qualitatively identical, although the critical coupling for the metal-insulator transition (MIT) in the SB theory is greatly increased at small V due to the much smaller excitonic renormalization of the hybridization than at $\epsilon_f=0$.

The $t_{ff}=0.01$ data illustrate the behavior of the EFKM when the noninteracting system is insulating. The system remains in the ECI state for all G, and there are no significant differences between these results and those presented in Sec. III B. More interesting is the case $t_{ff}=0.1$ as there is a second-order MIT at $G\approx 0.2W$. This is reflected in the abrupt change in the first derivative with respect to G of the curves in Fig. 7. Because the MIT is driven by the excitonic renormalization of the hybridization, which follows closely the HF values in the insulating state, the SB and HF results for the critical coupling agree very well. Since the effective hybridization in the SB theory is always smaller than in the HF theory, however, the MIT occurs at a slightly higher value of G in the SB theory.

As t_{ff} is further increased, the MIT in the SB theory becomes first order. This case is represented in Fig. 7 by the $t_{ff}=0.5$ results. Note that there is a region around $G=0.7W$ where both the ECI and M phases are solutions to Eq. (27). Within the ECI phase, the SB and HF results are in close agreement for d, s_b, and ΔV; in the M phase, however, the two theories give very different predictions. This is due to the much smaller effective hybridization within the SB theory [see Fig. 7(d)] as well as the importance of the strong correlations in the M phase. The latter aspect is clearly shown in Figs. 7(a) and 7(b) by the close correspondence between z^2 and d in the $V=0.05W$ and $V=0$ systems. Again, this is not seen in the G dependence of s_b due to the much greater sensitivity of s_b to the value of V. Note that as we lower G from the ECI phase and enter into the metastable regime, the band gap continuously vanishes as we approach the limit of metastability. Increasing G from within the M state, however, the band overlap does not go to zero as the metastable limit is approached.

We present the phase diagram for the EFKM with $t_{ff}<0$ at $V=0.05W$ and $\epsilon_f=0$ in Fig. 8. The phase boundaries in both the SB and HF theories are included. In the HF theory, we find only a line of second-order transitions. For the SB theory, the MIT is of second order for $t_{ff}\lesssim 0.11$ and is of first order at higher values of t_{ff}, where a region with both M and ECI solutions is found. As in the previous phase diagrams, the metastable phase is given in brackets. The origin of the first-order MIT in the SB theory is related to the behavior of the EFKM in the limit $t_{ff}=1$. Here, the SB solution of the EFKM with $V\neq 0$ is identical to the paramagnetic SB solution of the Hubbard model in a transverse magnetic field, so for sufficiently small V, there is a first-order transition into the FB state and a region of both M and FB solutions. As t_{ff} is reduced from unity, this region narrows until the lines of metastability converge at $t_{ff}\approx 0.11$.

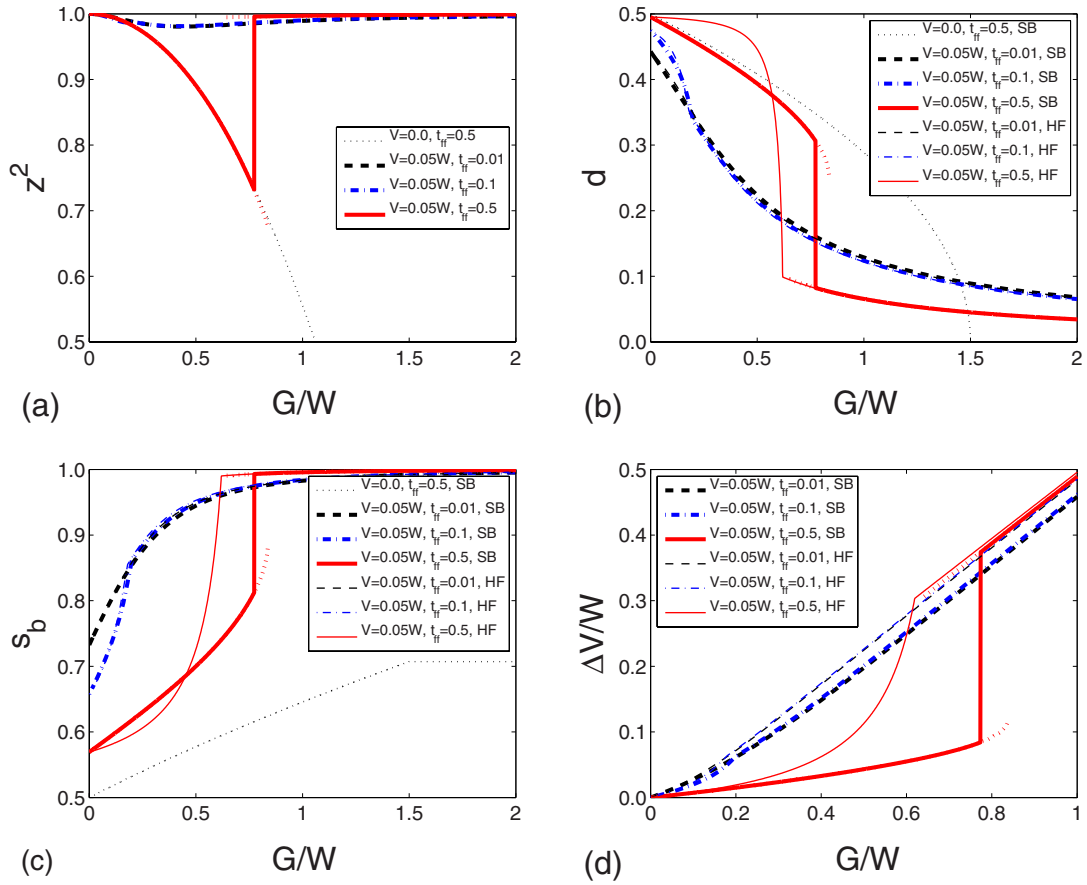

FIG. 7. (Color online) Variation of the SB parameters with G and t_{ff} for $V=0.05$ and $\epsilon_f=0$. In (b)–(d), thick lines indicate the SB solution, while the thin lines of the same style and color indicate the corresponding Hartree-Fock solution. For the $t_{ff}=0.5$, $V=0.05W$ SB result, the metastable solution is given by the thick dotted line. (a) Band-renormalization factor z^2. (b) SB field d. (c) SB field s_b. (d) Change in hybridization ΔV.

D. Excitonic insulator

As noted in Sec. III B, the SB theory only allows an EI phase at $\epsilon_f=0$, whereas the EI phase is a ubiquitous feature of the HF solution. As can be seen in Fig. 9, at $\epsilon_f=0$, the two theories are in close agreement for the excitonic average Δ when $G>W$ or $V\gtrsim 0.1W$; for $V\ll 0.1W$ and $G<W$, the SB theory predicts a smaller $|\Delta|$ than in the HF theory, as expected from the smaller values of the effective hybridization [see Fig. 4(d)]. The predictions of the HF and SB theories diverge considerably for $\epsilon_f\neq 0$ as displayed in Fig. 9(b). Note that in the HF theory, Δ is almost identical for $\epsilon_f=0$ and $\epsilon_f=0.05W$. The very different results of the HF and SB mean-field approaches suggest separate interpretations of the EI phase.

In the HF theory, the EI phase arises from the formation of an excitonic condensate due to the attraction between f holes and c electrons. This excitonic pairing creates an effective hybridization between the two bands, as an electron can hybridize from a c orbital into an f orbital via the formation and dissociation of an exciton. At $T=0$, the normal (N) state is unstable to the EI phase if the effective hybridization is sufficient to open a gap in the system. In particular, the EFKM with $t_{ff}\leqslant 0$ has an instability toward the EI phase for arbitrarily small interorbital Coulomb repulsion G. For t_{ff}

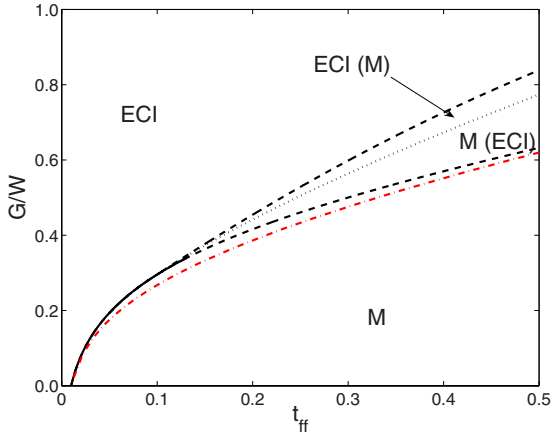

FIG. 8. (Color online) Phase diagram in the G-t_{ff} plane for $V=0.05W$ and $\epsilon_f=0.0$. The red dot-dash line gives the second-order boundary between the ECI and M phases in the Hartree-Fock theory. Within the slave-boson theory, the ECI and M phases are separated by a second-order transition at $t_{ff}\lesssim 0.12$ (black solid line). At higher values of t_{ff}, the transition is first order, with the black dashed lines showing the limits of metastability of the ECI and M phases. The two phases have equal energy along the dotted line; the metastable phase is indicated in brackets.

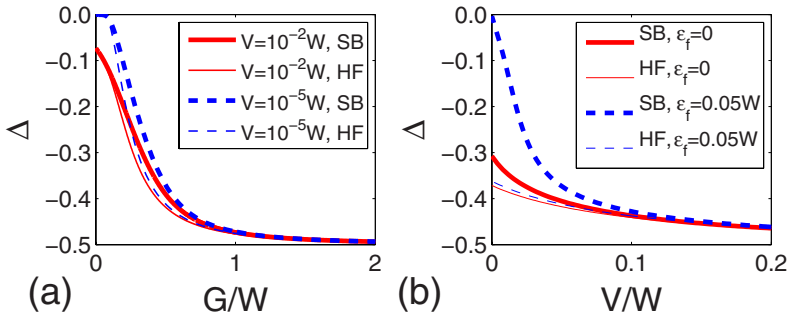

FIG. 9. (Color online) (a) Excitonic average as a function of G for the SB and HF theories at $t_{ff}=-0.1$ and $\epsilon_f=0$. (b) V dependence of the excitonic average Δ for the HF and SB theories at $t_{ff}=-0.1$ and $G=0.4W$. In both panels, the thick lines indicate the SB solution, while the thin lines of the same style and color indicate the corresponding Hartree-Fock solution.

>0, however, the EI phase is only realized when the effective hybridization is large enough to eliminate the band overlap, and so the N phase is stable up to a finite critical interaction strength.

To understand the results of the SB theory, we note that the a-b basis introduced in Eq. (2) rewrites the Hamiltonian in terms of bonding and antibonding orbitals at each site. The EI phase occurs when these orbitals have mixed c and f character in the $V\to 0$ limit. In the noninteracting system, this condition is only satisfied for $\epsilon_f=0$ when the transformation to the a-b basis is independent of V [see Eq. (2)]. For $\epsilon_f\neq 0$, in contrast, the transformation to the a-b basis is V dependent and the bonding and antibonding orbitals continuously evolve into the $V=0$ atomic orbitals as $V\to 0$. Due to the mixture of the two atomic orbitals in the a-b basis, at finite G, the Coulomb-induced splitting of the bonding and antibonding orbitals produces the enhancement of the hybridization given by Eq. (28). This induced hybridization only survives in the $V\to 0$ limit when $\epsilon_f=0$, as it is only in this case that the atomic orbitals are equally mixed in the a-b basis for all V. As such, we obtain a spontaneous hybridization when $\epsilon_f=0$, whereas for $\epsilon_f\neq 0$, the system continuously evolves into the $V=0$ system as clearly evidenced by the phase diagram in Fig. 6.

The $\epsilon_f=0$ ground state phase diagram of the EFKM for $-1\leqslant t_{ff}\leqslant 1$ is presented in Fig. 10. Again, we plot the phase diagram for both the HF and SB theories. For the HF theory, the second-order MIT at $t_{ff}>0$ found in Sec. III C remains. Although the band gap vanishes continuously as we approach the metallic state from within the EI phase, the excitonic average Δ discontinuously drops to zero at this line, and so below it, the system is in the N state. In contrast to the HF results, the SB theory predicts a first-order MIT for all $t_{ff}>0$ in the limit of vanishing hybridization. As in Sec. III C, the lower limit of metastability of the EI phase lies just above the MIT in the HF theory, and the band gap continuously vanishes as the line of metastability is approached, but Δ tends to a finite value. A finite band overlap is always found as we approach the upper limit of metastability from within the N phase. Of particular note is the t_{ff} dependence of this line: for sufficiently large t_{ff}, the boundary is given by $G=(1+t_{ff})W$, which corresponds to the limit of metastability of the metallic phase at $\epsilon_f=0^+$ found in Sec. III A. At $t_{ff}\approx 0.1$, however, there is an abrupt change in this line, with the limit of metastability of the N phase converging to $G=0$ at $t_{ff}=0$.

IV. CONCLUSIONS

In this work, we have studied the EFKM within the SB mean-field theory introduced by Kotliar and Ruckenstein.[20] For the system with $V\neq 0$, we have compared the predictions of SB theory to those of the standard HF approach.[6] We have found that for the EFKM with $V=0$, the SB phase diagram displays strong similarities to the SB solution of the paramagnetic Hubbard model. In particular, at $\epsilon_f=0$, we find a transition into a Brinkman-Rice-like insulating state as G is increased, while at small finite ϵ_f, there is a first-order valence transition. For finite V, a distinction between the EFKM with $t_{ff}\leqslant 0$ and $t_{ff}>0$ must be made. In the former case, the model is always in an insulating state and there is a considerable renormalization of the hybridization by the Coulomb interaction. For $\epsilon_f=0$, the SB and HF results are in good agreement, whereas for $\epsilon_f\neq 0$, the SB and HF theories only coincide when $V\gg|\epsilon_f|$. For $V\ll|\epsilon_f|$, the SB theory displays a crossover between a state with strong correlations beyond the HF level at $G\ll W$ and an excitonically correlated state at $G\gtrsim W$. At sufficiently large $t_{ff}>0$, both the HF and SB theories predict a MIT as G is increased. In the former,

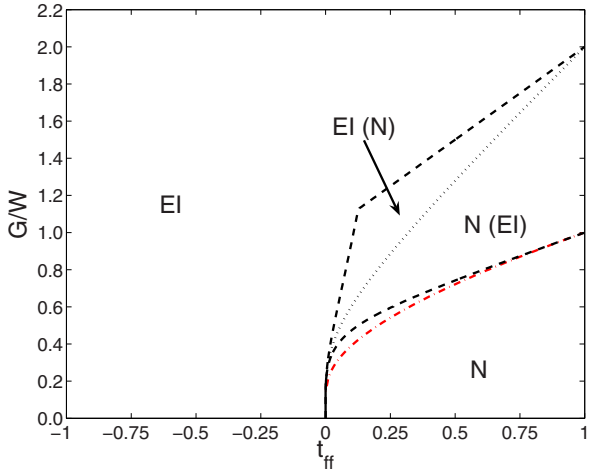

FIG. 10. (Color online) $V=0$ phase diagram in the G-t_{ff} plane for $\epsilon_f=0.0$. The red dot-dash line indicates the MIT between the EI and N phases in Hartree-Fock theory. The slave-boson theory predicts a first-order MIT between the EI and N phases, with the boundaries of metastability given by the dashed lines. The N and EI phases have equal energy along the dotted line; the metastable phase is indicated in brackets.

this is always of second order; for the latter, the MIT is of first order for t_{ff} greater than some critical value. The presence of first-order transitions in our SB treatment suggests that it is worthwhile to include the interorbital Coulomb repulsion as an important factor in discontinuous valence transitions.

We have also studied the appearance of an EI phase within the EFKM, and our conclusions severely constrain the parameter space of the model where such a state is possible. In contradiction to the results of HF theory where the EI phase is a ubiquitous feature of the $T=0$ phase diagram,[5,13] the SB theory only predicts a spontaneous hybridization when the c- and f-electron atomic orbitals are degenerate, i.e., $\epsilon_f=0$. When $\epsilon_f \neq 0$, the effective hybridization continuously vanishes as $V \rightarrow 0$. We have explained this difference in terms of the importance of the bonding and antibonding orbitals in the SB theory. This imposes a condition on the atomic structure for the realization of the EI phase. Such a condition is absent in the HF theory.

Our work has only considered uniform ground states of the EFKM. From the rigorous solution of the FKM, it is expected that the EFKM on a bipartite lattice has an instability toward a density-wave state at $\epsilon_f=0$.[3] As demonstrated by a number of authors, this density-wave state is stable at $T=0$ and prevents the EI phase from being realized.[16,17,24] It is likely that this density-wave phase would also be found within a SB treatment of the model. As the condition for the EI phase in the SB theory concerns only the atomic as opposed to the band structure, however, the EI phase could still be realized in systems where the mean-field density-wave state is unstable, e.g., frustrated lattices. It would also be of interest to examine the effect of doping away from half-filling.

The addition of spin is a necessary step in relating the EFKM to realistic systems. Since the EFKM was first developed with valence transition physics in mind, the natural way to include spin is to take the periodic Anderson model and add a c-f Coulomb repulsion. Such a model has been studied by several authors.[25] In these works, however, the c-f interaction is treated using a Hubbard-Stratonovich decoupling, while the f-f repulsion is examined using the Coleman slave-boson technique.[26] It is, therefore, of interest to treat both interactions on an equal footing; as the atomic Hamiltonian of the periodic Anderson model with c-f interaction cannot be easily diagonalized, however, this would require the use of the slave-boson technique proposed in Ref. 22.

ACKNOWLEDGMENTS

This work was funded by the European Union CoMePhS project. The author gratefully acknowledges H. Yamase and M. Gulácsi for many helpful discussions and their critical reading of the manuscript. K. I. Kugel is also thanked for useful discussions. The author is grateful to H. C. Lee for drawing his attention to the extension of the periodic Anderson model by c-f repulsion.

[1] L. M. Falicov and J. C. Kimball, Phys. Rev. Lett. **22**, 997 (1969); R. Ramirez and L. M. Falicov, Phys. Rev. B **3**, 2425 (1971).
[2] J. M. Lawrence, P. S. Riseborough, and R. D. Parks, Rep. Prog. Phys. **44**, 1 (1981).
[3] T. Kennedy and E. H. Lieb, Physica A **138**, 320 (1986); U. Brandt and R. Schmidt, Z. Phys. B: Condens. Matter **63**, 45 (1986).
[4] M. Avignon and S. K. Ghatak, Solid State Commun. **16**, 1243 (1975); K. Kanda, M. Machida, and T. Matsubara, *ibid.* **19**, 651 (1976).
[5] A. N. Kocharyan and D. I. Khomskii, Sov. Phys. JETP **44**, 4040 (1976); D. I. Khomskii, Sov. Phys. Usp. **22**, 879 (1979).
[6] H. J. Leder, Solid State Commun. **27**, 579 (1978).
[7] E. Baeck and G. Czycholl, Solid State Commun. **43**, 89 (1982).
[8] L. V. Keldysh and Y. V. Kopaev, Sov. Phys. Solid State **6**, 2219 (1965).
[9] J. des Cloizeaux, J. Phys. Chem. Solids **26**, 259 (1965).
[10] T. M. Rice, Phys. Rev. B **2**, 3619 (1970); N. I. Kulikov and V. V. Tugushev, Sov. Phys. Usp. **27**, 954 (1984); E. Fawcett, H. L. Alberts , V. Yu. Galkin, D. R. Noakes, and J. V. Yakhmi, Rev. Mod. Phys. **66**, 25 (1994).
[11] D. V. Efremov and D. I. Khomskii, Phys. Rev. B **72**, 012402 (2005).
[12] P. Wachter, B. Bucher, and J. Malar, Phys. Rev. B **69**, 094502 (2004); P. Wachter, A. Jung, and F. Pfuner, Phys. Lett. A **359**, 528 (2006).
[13] T. Portengen, Th. Östreich, and L. J. Sham, Phys. Rev. Lett. **76**, 3384 (1996); Phys. Rev. B **54**, 17452 (1996).
[14] P. Farkašovský, Phys. Rev. B **59**, 9707 (1999); **65**, 081102(R) (2002).
[15] V. Zlatić, J. K. Freericks, R. Lemański, and G. Czycholl, Philos. Mag. B **81**, 1443 (2001).
[16] G. Czycholl, Phys. Rev. B **59**, 2642 (1999).
[17] P. M. R. Brydon, J.-X. Zhu, M. Gulácsi, and A. R. Bishop, Phys. Rev. B **72**, 125122 (2005).
[18] C. D. Batista, Phys. Rev. Lett. **89**, 166403 (2002); C. D. Batista, J. E. Gubernatis, J. Bonca, and H. Q. Lin, *ibid.* **92**, 187601 (2004).
[19] L. G. Sarasua and M. A. Continentino, Phys. Rev. B **69**, 073103 (2004).
[20] G. Kotliar and A. E. Ruckenstein, Phys. Rev. Lett. **57**, 1362 (1986).
[21] H. Kusunose, S. Yotsuhashi, and K. Miyake, Phys. Rev. B **62**, 4403 (2000); A. Rüegg, M. Indergand, S. Pilgram, and M. Sigrist, Eur. Phys. J. B **48**, 55 (2005).
[22] F. Lechermann, A. Georges, G. Kotliar, and O. Parcollet, Phys. Rev. B **76**, 155102 (2007).
[23] D. Vollhardt, Rev. Mod. Phys. **56**, 99 (1984).
[24] P. Farkašovský, Z. Phys. B: Condens. Matter **104**, 553 (1997); Phys. Rev. B **70**, 035117 (2004).
[25] Y. Onishi and K. Miyake, J. Phys. Soc. Jpn. **69**, 3955 (2000); C. Pépin, Phys. Rev. Lett. **98**, 206401 (2007); H. C. Lee, Physica B (to be published).
[26] P. Coleman, Phys. Rev. B **29**, 3035 (1984); **35**, 5072 (1987).